



OPEN UF-5000 urinary erythrocyte parameters versus urinary aberrant erythrocytes and acanthocytes for diagnosing IgA glomerular hematuria

Shuangshuang Lv[✉], Yi Fang, Xiaxuan Hu, Jian Zhang, Xinxin Lou, Caihong Chen, Lijiao Cao & Dongmei Zhang

This study evaluated the diagnostic value of the automated UF-5000 parameters and compared it with that of aberrant erythrocytes and acanthocytes classified by microscopy for identifying IgA glomerular hematuria to propose a predictive model for clinical use. It also compared correlations between erythrocyte parameters and malformed erythrocytes. Urine samples from 53 biopsy-proven IgA hematuria cases and 143 non-IgA nephropathic hematuria cases as controls were analyzed. The ratio of small red blood cells to nonlysed red blood cells (UF-sRBC%) and lysed red blood cells (lysed RBCs) showed good diagnostic performance for IgA glomerular hematuria (area under the curve [AUC] = 0.857 [$P = 0.000$] and AUC = 0.860 [$P = 0.000$], respectively). Combining UF-sRBC%, lysed RBCs, and urine protein dry chemistry improved the diagnostic accuracy (AUC = 0.967; positive predictive value [PPV] = 91.89%; negative predictive value [NPV] = 93.10%; $P = 0.000$). This approach surpassed traditional microscopy for aberrant erythrocytes (AUC = 0.895; PPV = 62.27%; NPV = 88.66%; $P = 0.008$) and acanthocytes (AUC = 0.868; PPV = 72.97%; NPV = 83.65%; $P = 0.006$). The erythrocyte size index was negatively correlated with the proportion of urinary aberrant erythrocytes ($r = -0.787$; $P = 0.000$). The UF-5000 erythrocyte parameters facilitate rapid identification of IgA nephropathy and could replace manual microscopy.

Keywords Hematuria, IgA nephropathy, Microscopy, Erythrocytes, Acanthocytes

IgA nephropathy (IgAN), which is characterized by IgA deposits in the glomerular tunica albuginea, is the most prevalent form of primary glomerulonephritis worldwide and poses a significant risk of chronic renal failure¹. The clinical presentations of IgAN include asymptomatic with microscopic hematuria and/or visible intermittent hematuria as well as stable renal function or rapidly progressive glomerulonephritis^{2–5}. Hematuria is the most common clinical manifestation at all stages of IgAN⁶. Recent studies have indicated that hematuria with IgAN occurs as a result of inflammatory glomerular injury caused by pathogenic events that drive disease progression^{7,8}. Therefore, utilizing hematuria for the differential diagnosis of IgAN has significant clinical utility.

The presence of aberrant red blood cells (RBCs), especially acanthocytes, detected using urine microscopy is a recognized marker of glomerular injury⁹. Several studies have explored the definitions and thresholds of aberrant erythrocytes and acanthocytes to detect renal hemorrhage with IgAN and other conditions; however, the sensitivity of these studies varied, and they did not provide novel findings^{10–12}. Manual classification of urinary erythrocytes using microscopy is time-consuming, labor-intensive, and prone to individual variability between observers, thus hindering standardization⁶. Additionally, erythrocyte morphology is affected by various factors, including centrifugation^{13,14}.

UF-5000 (Sysmex Corporation, Kobe, Japan) is a fully automated urine sediment analyzer that is widely used in clinical laboratories to assess urine components. Based on the fluorescence flow cytometry method, UF-5000 quickly and efficiently identifies and classifies urinary component fractions and provides standardized information regarding RBCs, specifically nonlysed RBCs (NLRBCs), lysed RBCs, large RBCs, small RBCs, and 70% of the RBC forward scattered light intensity (RBC-P70Fsc; an indicator of the erythrocyte size), the intensity

Clinical Laboratory, Dongyang People's Hospital, No. 60 Wuning West Road, Dongyang City 322100, Zhejiang, China. ✉email: 15958490336@139.com

distribution of forward scattered light of erythrocytes (RBC-Fsc-DW; an indicator of erythrocyte morphologic diversity), and erythrocyte information prompts (RBC-info)¹⁵. Some studies have confirmed that the erythrocyte parameters provided by UF-5000 have good diagnostic value for glomerulonephritic hematuria^{13,16}. Specifically, UF-%sRBCs (UF-%sRBCs=[small RBCs/NLRBCs ×100%]) and lysed RBCs were highly correlated with glomerulonephritis; additionally, UF-%sRBCs were highly correlated with the presence of aberrant RBCs¹³. UF-5000 exhibited better diagnostic consistency (98.5% sensitivity for RBCs) than that of manual microscopy¹⁷. However, the diagnostic value of the erythrocyte parameters of IgA glomerular hematuria provided by UF-5000 has been insufficiently studied, and comparisons between these parameters and manually categorized aberrant erythrocytes and acanthocytes have been rarely reported. Therefore, this study aimed to evaluate the diagnostic value of the automated erythrocyte parameters of UF-5000 and compare it with that of aberrant erythrocytes and acanthocytes classified by microscopy for the identification of IgA glomerular hematuria. It also compared correlations between the RBC parameters of UF-5000 and abnormal erythrocytes and acanthocytes classified by microscopy to provide a basis for the objective and standardized application of these parameters for the clinical diagnosis and treatment of IgA glomerular hematuria. Additionally, we aimed to develop a predictive model for IgA glomerular hematuria by combining erythrocyte parameters with urine protein dry chemistry, thus offering a novel perspective regarding the diagnosis and treatment of this disease.

Results

One-way comparative analysis

Regarding the erythrocyte parameters of UF-5000, the mean (\pm standard deviation [SD]) of the erythrocyte volume parameter RBC-P70Fsc of the control group was significantly higher (108.38 ± 26.14 ch; ch is a unit of measurement that reflects the intensity of a forward scattered light signal) than that of the IgA glomerular hematuria group (79.25 ± 19.64 ch; $P=0.000$) (Fig. 1A; Table 1). The median small RBC count and median lysed RBC count of the IgA glomerular hematuria group were $91.15/\mu\text{L}$ (interquartile range [IQR], 35.80–230.18) and $12.50/\mu\text{L}$ (IQR, 4.88–18.20), respectively; these values were higher than those of the control group ($23.40/\mu\text{L}$ [IQR, 13.30–52.80; $P=0.003$] and $0.90/\mu\text{L}$ [IQR, 0.30–3.40; $P=0.000$], respectively) (Fig. 1D and F; Table 1). Additionally, the mean (\pm SD) of UF-sRBC% (small RBCs \times 100%/NLRBCs; $0.67\% \pm 0.16\%$) and UF- lysed RBC% (lysed RBCs \times 100%/NLRBCs; $0.11\% \pm 0.12\%$) were higher than those of the control group ($0.36\% \pm 0.24\%$ [$P=0.000$] and $0.03 \pm 0.05\%$ [$P=0.000$], respectively) (Fig. 1G and H; Table 1). There were no significant differences in RBC-Fsc-DW ($P=0.108$), large RBCs ($P=0.153$), and NLRBCs ($P=0.514$) between the two groups (Fig. 1B, C, E). In the IgA glomerular hematuria group, 14 (26.42%) cases, 0 (0.00%) cases, and 39 (73.58%) cases exhibited dysmorphic-type RBCs, isomorphic-type RBCs, and mixed-type RBCs, respectively. In comparison, in the control hematuria group, 7 (4.90%) cases, 43 (30.07%) cases, and 93 (65.03%) cases exhibited dysmorphic-type RBCs, isomorphic-type RBCs, and mixed-type RBCs, respectively. The difference between these two groups was statistically significant ($P=0.000$) (Table 1).

Among other indexes, the proportion of urinary aberrant RBCs, acanthocytes, serrated RBCs, ring forms, micro-RBCs classified by microscopy, and blood creatinine and urea nitrogen levels of the IgA glomerular hematuria group were higher than those of the control group; however, the estimated glomerular filtration rate of the control group was significantly higher than that of the IgA glomerular hematuria group, and the difference was statistically significant. The positive rates of the urine protein grades were higher than those of those of control group ($P=0.000$ for all) (Table 1).

Logistic multifactor analysis

A multifactorial regression analysis that combined erythrocyte information parameters with urine protein dry chemistry revealed that lysed RBCs ($P=0.008$; odds ratio [OR]=1.321; 95% confidence interval [CI]: 1.108–1.574), UF-sRBC% ($P=0.002$; OR=1.062; 95% CI: 1.031–1.094), and urine protein ($P=0.000$; OR=5.562; 95% CI: 2.873–10.767) were risk factors for glomerular hematuria with IgA (Fig. 2). These indicators were included in a prediction model for the receiver-operating characteristic (ROC) curve analysis.

ROC curve analysis

According to the ROC curve analysis that compared the IgA glomerular hematuria group with the control hematuria group, UF-sRBC% ($\geq 42.24\%$), lysed RBCs ($\geq 3.55/\mu\text{L}$), and urinary protein ($\geq 1+$) yielded the largest areas under the ROC curve (AUCs) for identifying IgA glomerular hematuria (AUC=0.967; $P=0.000$; 95% CI: 0.942–0.992) with the highest sensitivity (97.7%), specificity (84.8%), positive predictive value (PPV; 91.89%), and negative predictive value (NPV; 93.10%). Thereafter, the proportion of aberrant RBCs% (microscopy) identified by manual microscopy had a cutoff value of 63.5% (AUC=0.895; $P=0.000$; 95% CI: 0.847–0.942), with sensitivity of 86.40%, specificity of 83.30%, PPV of 67.27%, and NPV of 88.68%. Urine protein (AUC=0.881; $P=0.000$; 95% CI: 0.809–0.953) with a cutoff value of 1+ showed sensitivity of 77.30%, specificity of 96.40%, PPV of 87.18%, and NPV of 93.00%. UF-sRBC%+ lysed RBCs (AUC=0.879; $P=0.000$; 95% CI: 0.831–0.927) exhibited sensitivity of 77.30%, specificity of 96.40%, PPV of 87.18%, and NPV of 93.00%. The percentage of acanthocytes (acanthocytes%) (microscopy) (AUC=0.868; $P=0.000$; 95% CI: 0.805–0.932) with a cutoff value of 2.5% exhibited sensitivity of 84.10%, specificity of 83.30%, PPV of 72.97%, and NPV of 83.65%. lysed RBCs (UF-5000) (AUC=0.860; $P=0.000$; 95% CI: 0.797–0.923) with a cutoff value of $3.55/\mu\text{L}$ showed sensitivity of 79.50%, specificity of 82.60%, PPV of 63.647%, and NPV of 75.14%. UF-sRBC% (UF-5000) (AUC=0.857; $P=0.000$; 95% CI: 0.804–0.910) with a cutoff value of 42.24% showed sensitivity of 97.70%, specificity of 68.80% PPV of 55.567%, and NPV of 81.46% (Table 2).

However, only the urine protein + UF-sRBC%+lysed RBCs model showed statistically significant differences in the AUCs among the erythrocyte parameters of UF-5000 when compared with the urinary aberrant RBCs%

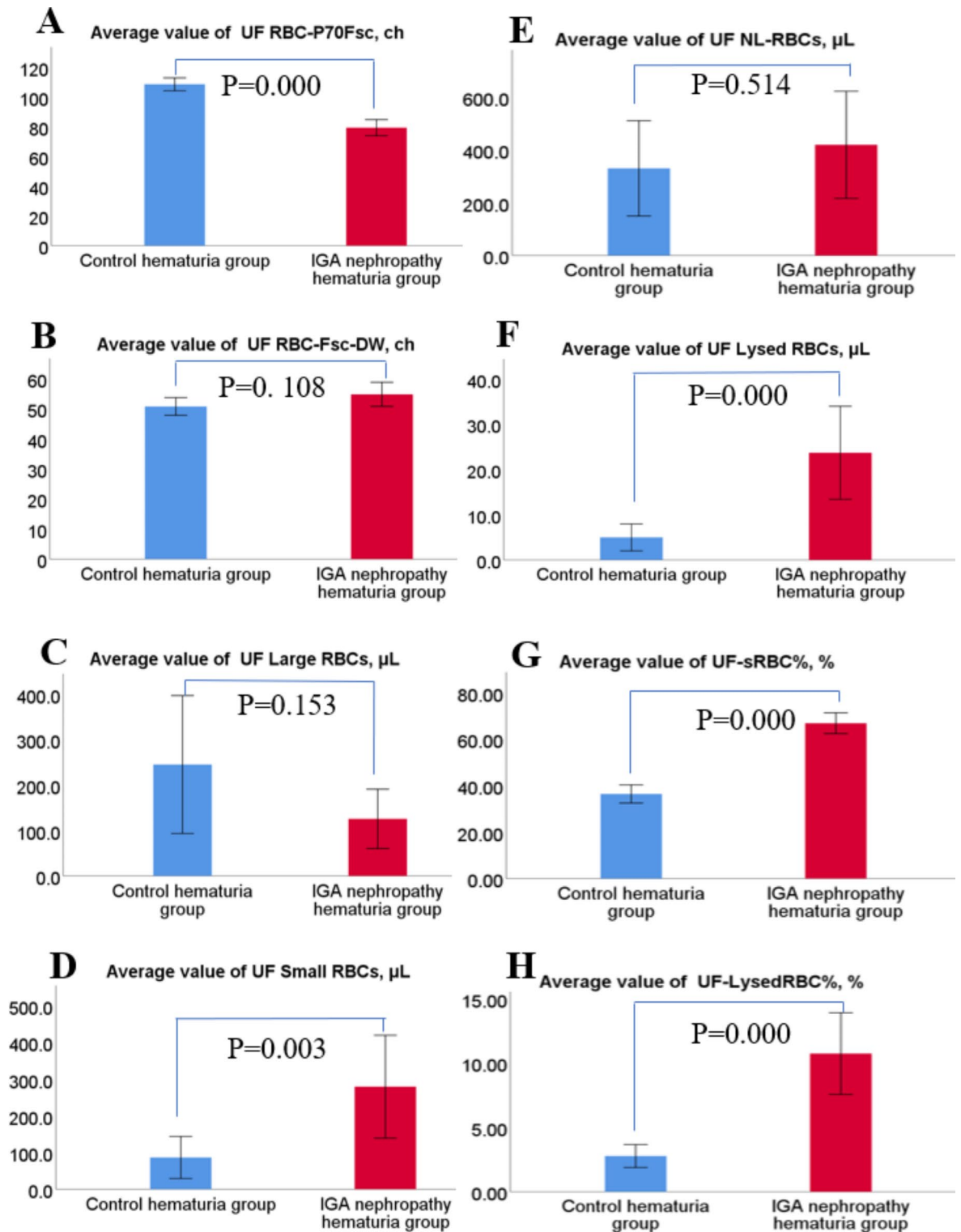


Fig. 1. Bar graph of differences in UF-5000 erythrocyte information parameters between the two groups. Small red blood cells (RBCs), lysed RBCs, UF-sRBC% (small RBCs \times 100%/nonlysed RBCs [NLRBCs]), and UF-lysed RBC% (lysed RBCs \times 100%/NLRBCs) of the IgA glomerular hematuria group were higher than those of the control hematuria group. The erythrocyte volume parameter, RBC-P70Fsc, of the control hematuria group was significantly higher than that of the IgA glomerular hematuria group ($P < 0.05$). The erythrocyte distribution index, RBC-Fsc-DW, large RBCs, and NLRBCs were not statistically different between groups ($P > 0.05$).

Factor	IgA nephropathy group (n = 53)	Control group (n = 143)	P
Sex (F/M), n	32/21	93/50	0.547
Age (years), mean \pm SD	45.66 \pm 15.70	46.17 \pm 16.24	0.840
UF-5000 red blood cell parameters			
RBC-Info, n	53	143	0.000**
Isomorphic type RBC, n (%)	0 (0)	43 (30.07)	0.000**
Dysmorphic type RBC, n (%)	14 (26.42)	7 (4.90)	0.000**
Mixed type RBC, n (%)	39 (73.58)	93 (65.03)	0.000**
RBC-P70Fsc (ch), mean \pm SD	79.25 \pm 19.64	108.38 \pm 26.14	0.000**
RBC-Fsc-DW (ch), mean \pm SD	54.74 \pm 14.49	50.71 \pm 17.76	0.108
Large RBCs (/ μ L), median (IQR)	37.05 (14.45–99.90)	47.10 (23.41–79.10)	0.153
Small RBCs (/ μ L), median (IQR)	91.15 (35.80–230.18)	23.40 (13.30–52.80)	0.003**
NL-RBCs (/ μ L), median (IQR)	159.81 (66.00–335.65)	76.70 (38.20–126.80)	0.514
Lysed RBCs (/ μ L), median (IQR)	12.50 (4.88–18.20)	0.90 (0.30–3.40)	0.000**
UF-sRBC% (%), mean \pm SD	0.67 \pm 0.16	0.36 \pm 0.24	0.000**
UF-Lysed RBC% (%), mean \pm SD	0.11 \pm 0.12	0.03 \pm 0.05	0.000**
Phase contrast microscopy			
Total RBCs(/ml), median (IQR)	5.90 (15.80–40.00)	6.97 (3.40–17.30)	0.294
Aberrant RBCs% (%), mean \pm SD	68.43 \pm 14.67	32.41 \pm 22.22	0.000**
Acanthocytes% (%), mean \pm SD	9.57 \pm 9.48	1.05 \pm 2.15	0.000**
Serrated RBCs% (%), mean \pm SD	12.15 \pm 8.97	3.72 \pm 5.44	0.000**
Ring Forms% (%), mean \pm SD	10.32 \pm 9.05	3.42 \pm 5.53	0.000**
Ghost Cells% (%), mean \pm SD	4.53 \pm 7.59	3.17 \pm 4.75	0.136
Fragments% (%), mean \pm SD	0.40 \pm 1.12	0.51 \pm 1.41	0.555
Micro RBCs% (%), mean \pm SD	31.47 \pm 9.21	20.54 \pm 16.62	0.000**
Serum biochemical tests			
Serum BUN (mmol/L), mean \pm SD	6.87 \pm 4.21	5.14 \pm 0.88	0.000**
Serum creatinine (μ mol/L), mean \pm SD	131.28 \pm 165.71	63.85 \pm 14.94	0.000**
eGFR (ml/min/1.73 m ²), mean \pm SD	92.16 \pm 32.1	105.22 \pm 17.25	0.000**
UC-3500 Urine Dry Chemistry Test			
Urinary dipstick scores of protein, n	44	138	0.000**
Negative, n (%)	6 (13.64)	84 (60.87)	0.000**
Weak positive, n (%)	4 (9.09)	49 (35.51)	0.000**
1+, n (%)	12 (27.28)	5 (3.62)	0.000**
2+, n (%)	8 (18.18)	0 (0)	0.000**
3+, n (%)	9 (20.45)	0 (0)	0.000**
4+, n (%)	5 (11.36)	0 (0)	0.000**

Table 1. Demographic and laboratory parameters of IgA renal hematuria and control. Normally distributed variables are summarized as mean \pm SD, and non-normally distributed variables are summarized as median (Q1–Q3, interquartile range); Aberrant RBCs% = sum of the number of acanthocytes, serrated RBCs, ring forms, ghost cells, fragments, and micro erythrocytes /total number of erythrocytes * 100%; Acanthocytes%= acanthocytes/total number of erythrocytes * 100%;NL-RBC, non-lysed RBC; UF-sRBC%, Small RBCs/NL-RBCs* 100%; UF-Lysed RBC% ,Lysed RBCs/NL-RBCs* 100%; Ch, a unit of measurement used to measure the intensity of a forward scattering light signal; eGFR, estimated glomerular filtration rate; ** $P < 0.01$; * $P < 0.05$.

and acanthocytes%, which are useful for identifying IgA glomerular hematuria ($P = 0.008$ and $P = 0.006$, respectively) (Fig. 3).

Correlation analysis

The percentage of aberrant RBCs (aberrant RBCs%) was negatively correlated with RBC-P70Fsc ($r = -0.787$; $P = 0.000$). The aberrant RBCs% was positively correlated with UF-sRBC% ($r = 0.603$; $P = 0.002$) (Fig. 4A). The acanthocytes% was positively correlated with UF- lysed RBC% ($r = 0.657$; $P = 0.000$). The acanthocytes% was negatively correlated with RBC-P70Fsc ($r = -0.549$; $P = 0.003$) (Fig. 4B).

Discussion

Hematuria assessments and urinary sediment microscopy are common tools used by nephrologists to evaluate glomerular disease. RBC casts and aberrant erythrocytes, especially acanthocytes (ring-shaped erythrocytes with protruding blisters), visualized using microscopy are well-recognized markers of glomerular injury⁹.

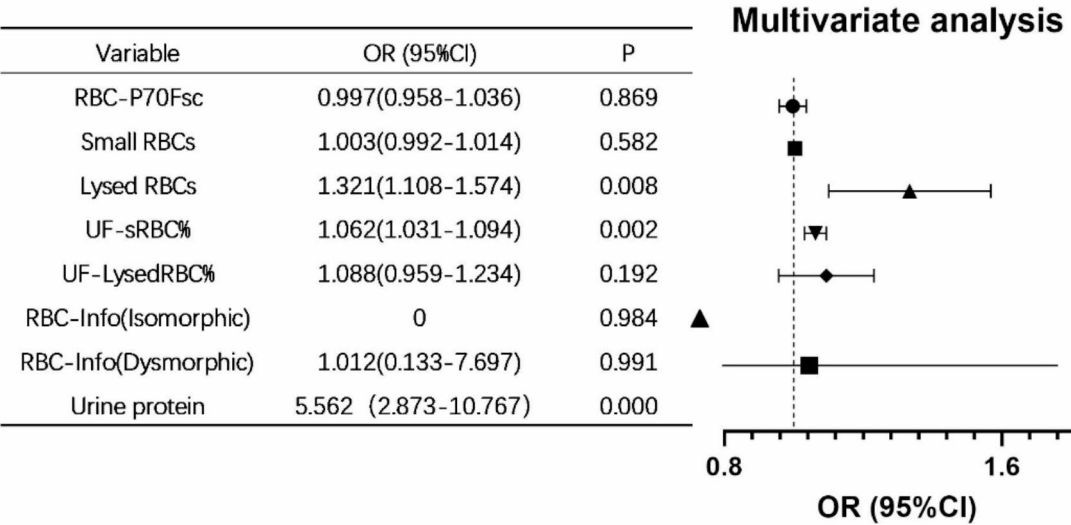


Fig. 2. Multifactor analysis chart. The multifactorial regression analysis combining erythrocyte information parameters with urine protein dry chemistry revealed that lysed RBCs, UF-sRBC, and urine protein were risk factors for renal hematuria in IgA nephropathies. *CI* confidence interval, *lysed RBC* lysed red blood cell, *OR* odds ratio, *RBC* red blood cell, *UF-sRBC* ratio of small red blood cells to nonlysed red blood cells.

The development of hematuria with IgAN may be associated with the deposition of immune complexes in the glomerular basement membrane, thus leading to ultrastructural abnormalities such as thinning and lamination^{5,18}. As erythrocytes traverse the damaged glomerular basement membrane, they undergo deformation to varying degrees; this deformation is exacerbated by the actions of urea, urease, and osmolality in the renal tubules, resulting in significant morphological changes such as prominent blisters^{19,20}. This explains why the urine aberrant erythrocytes and acanthocytes in this study were suitable for differentiating IgAN hematuria (AUC=0.895 and AUC=0.868, respectively; *P*=0.000). This finding was similar to that of Martinez et al., who reported that aberrant erythrocytes and acanthocytes classified by light microscopy and phase contrast microscopy could distinguish glomerular hematuria (AUC≥0.85; *P*<0.001).¹¹ Additionally, the cutoff values for the identification of IgA hematuria were 63.5% and 2.5% for urine aberrant erythrocytes and acanthocytes, respectively, in this study, which differed from the findings of Costa et al., who reported urinary aberrant erythrocyte and acanthocyte cutoff values of ≥70% and 5%, respectively, for the identification of glomerular hematuria^{21–23}. However, some studies have suggested that hematuria with more than 40% aberrant RBCs and/or more than 5% acanthocytes can be considered glomerulonephritis²⁴. Some studies reported that the cutoff value of aberrant RBCs using conventional microscopy and that of those using phase contrast microscopy for the identification of the source of hematuria were 22% and 40%, which were lower than our cutoff values; however, these were mainly used for glomerular hematuria, not for IgAN hematuria¹¹.

The UF-5000 fully automated urinary fraction analyzer utilizes fluorescence flow cytometry to measure urinary erythrocyte-related parameters; therefore, it has diagnostic value for glomerular hematuria^{13,16}.

Some studies reported that the erythrocyte parameters for UF-sRBC% and lysed RBCs may be suitable for glomerulonephritis, and that a good cutoff value for predicting glomerular hematuria can be obtained. The cutoff value of UF-sRBC% was 56.8%, (AUC=0.649; sensitivity, 94.1%; specificity, 38.1%; PPV, 68.3%; NPV, 82.1%), and the cutoff value for lysed RBCs was 4.6/μL (AUC=0.708; sensitivity, 82.4%; specificity, 56.0%; PPV, 72.60; NPV, 69.1%).¹³ During this study, we also found that UF-sRBC% was a good predictor of hematuria with IgAN (AUC=0.857; sensitivity, 97.70%; specificity, 68.80%; PPV, 55.56%; NPV, 81.46%) and lysed RBCs (AUC=0.860; sensitivity, 79.50%; specificity, 82.60%; PPV, 63.64%; NPV, 75.14%), and that UF-sRBCs (cutoff value, 42.24%) and lysed RBCs (cutoff value, 3.55/μL) had similar cutoff values.

By performing a comparison of instrumental parameters with microscopically classified malformed erythrocytes, we found that UF-sRBC% had high sensitivity of 97.7%, which was higher than that of microscopically classified aberrant erythrocytes; however, the specificity of UF-sRBC% was lower (68.8%) than that of aberrant erythrocytes (83.30%). The same was true for lysed RBCs, with sensitivity of 79.50% and specificity of 82.60%; both these values were lower than those of aberrant erythrocytes and acanthocytes (sensitivity, 84.10%; specificity, 83.3%). Both indicators did not outperform the recognized markers. However, we included the results of urine protein dry chemistry based on the insights of previous studies^{16,25,26}. We also found that when UF-sRBC% was ≥42.24%, the lysed RBC count was ≥3.55/μL, and urine proteins reached ≥1+, the sensitivity for identifying IgA glomerular hematuria was 97.70%, with specificity of 84.80% and notably higher PPV and NPV (91.89% and 93.10%, respectively) than those of other markers. This suggests that UF-sRBC% and


Factor	AUC	AUC bar chart	95% CI	P	Cutoff	Sensitivity	Specificity	Youden Index	PPV	NPV
Urine protein + UF-sRBC% +UF Lysed-RBCs	0.967		0.942–0.992	0.000**	–	97.70%	84.80%	0.825	91.89%	93.10%
Aberrant RBCs% , %	0.895		0.847–0.942	0.000**	≥ 63.5	86.40%	83.30%	0.697	67.27%	88.66%
Urinary dipstick scores of protein	0.881		0.809–0.953	0.000**	≥ 1+	77.30%	96.40%	0.736	87.18%	93.00%
UF-sRBC% +UF Lysed-RBCs	0.879		0.831–0.927	0.000**	–	97.70%	72.50%	0.702	61.36%	82.89%
Acanthocytes% , %	0.868		0.805–0.932	0.000**	≥ 2.5	84.10%	83.30%	0.674	72.97%	83.65%
UF Lysed-RBCs, /uL	0.860		0.797–0.923	0.000**	≥ 3.55	79.50%	82.60%	0.622	63.64%	75.14%
UF-sRBC% , %	0.857		0.804–0.910	0.000**	≥ 42.24%	97.70%	68.80%	0.666	55.56%	81.46%

Table 2. Comparison of the diagnostic performance of these parameters in the identification of IgA renal hematuria. Aberrant RBCs%(Microscopic), Proportion of malformed red blood cells in the urine to the total number of red blood cells; Acanthocytes%(Microscopic), Proportion of echinocytes to total red blood cells in the urine; UF-sRBC%, Small RBCs/NL-RBCs* 100%; ; Urine protein, Urinary dipstick scores of protein; AUC, area under the curve; CI, confidence interval; PPV, positive predictive value; NPV, negative predictive value; **, $P < 0.01$;*, $P < 0.05$.

lysed RBCs measured by the UF-5000 urine analyzer can help quickly identify IgA glomerular hematuria, thus providing a basis for clinical diagnosis and treatment.

Finally, we investigated the correlation between each erythrocyte parameter and manually categorized aberrant erythrocytes and acanthocytes. We observed a strong negative correlation between the RBC-P70Fsc, which represents the erythrocyte size index of UF-5000, and aberrant erythrocytes ($r = -0.787$; $P = 0.000$). This may be related to the changes in morphology and/or decreased hematocrit because most erythrocytes change after passing through the glomeruli and tubules^{9,27,28}. Normal RBCs have relatively regular morphology and a uniform size, and the forward scattered light intensity produced by them is relatively stable; therefore, the RBC-P70FSC parameters are also relatively stable. When the morphology of RBCs is abnormal, such as that of small RBCs, spinous RBCs, and broken RBCs, their size and shape change and the intensity of forward scattered light will change. For example, small RBCs, because of their smaller size, will weaken the intensity of forward scattered light, resulting in decreased RBC-P70FSC values. In contrast, spiny RBCs or other irregularly shaped and large RBCs increase the intensity of forward scattered light, resulting in increased RBC-P70FSC values¹⁵. Therefore, a change in this parameter may be useful to the clinical analysis of the source of hematuria.

Study limitations

This study had some limitations, such as incomplete inclusion criteria and insufficient data collection. Because of the insufficient number of IgA cases that underwent renal biopsy (53 patients with IgA in this study), we could not include more independent variables in the multifactorial regression analysis; therefore, important study factors were potentially missed. Furthermore, this study was limited to data from our hospital; therefore, the results represent the perspective of a single center rather than that of the entire region. In the future, we aim to address these limitations and enhance our research of these areas.

In conclusion, UF-5000 erythrocyte parameters of UF-sRBC% and lysed RBCs showed good diagnostic value for the identification of glomerular hematuria with IgA. Although not superior to traditional microscopic testing, testing that combined UF-sRBC%, lysed RBCs, and urine protein dry chemistry (with a cutoff value of 1+) greatly enhanced the diagnostic accuracy for IgA glomerular hematuria, thereby significantly outperforming the percentages of aberrant erythrocytes and acanthocytes detected by microscopy. The erythrocyte size index (RBC-P70Fsc) was highly negatively correlated with the proportion of urinary aberrant erythrocytes. The parameters of UF-5000 provide rapid identification of IgAN. Therefore, UF-5000 may be considered a substitute for manual

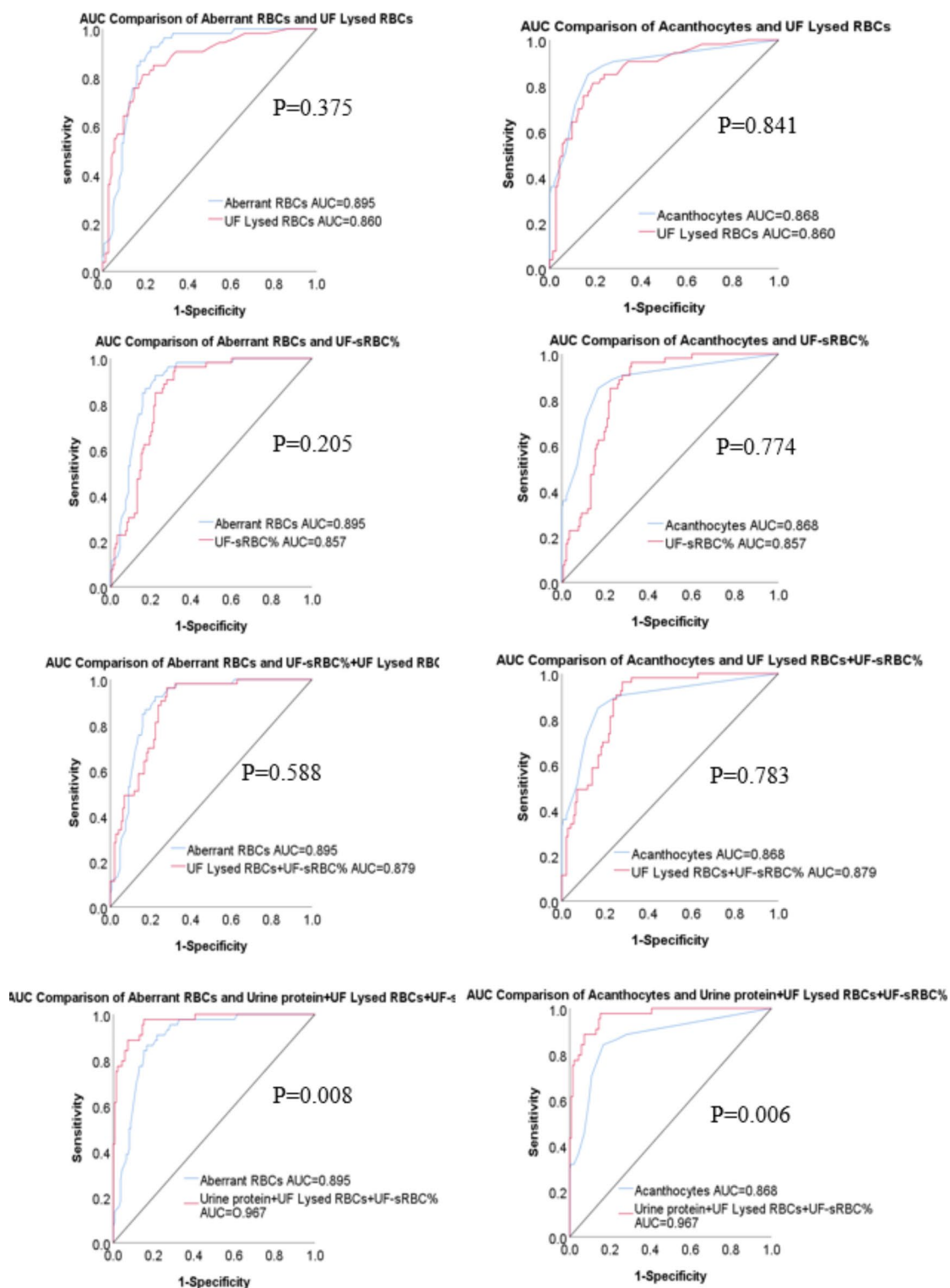


Fig. 3. Receiver-operating characteristic curve analysis. The urine protein + UF-sRBC%+lysed RBCs model showed statistically significant differences in the AUCs among the UF-5000 erythrocyte parameters when compared to the urinary aberrant RBCs% and acanthocytes% ($P=0.008$ and $P=0.006$, respectively). *AUC* area under the ROC curve, *lysed RBC* lysed red blood cell, *RBC* red blood cell, *ROC* receiver-operating characteristic, *UF-sRBC* ratio of small red blood cells to nonlysed red blood cells.

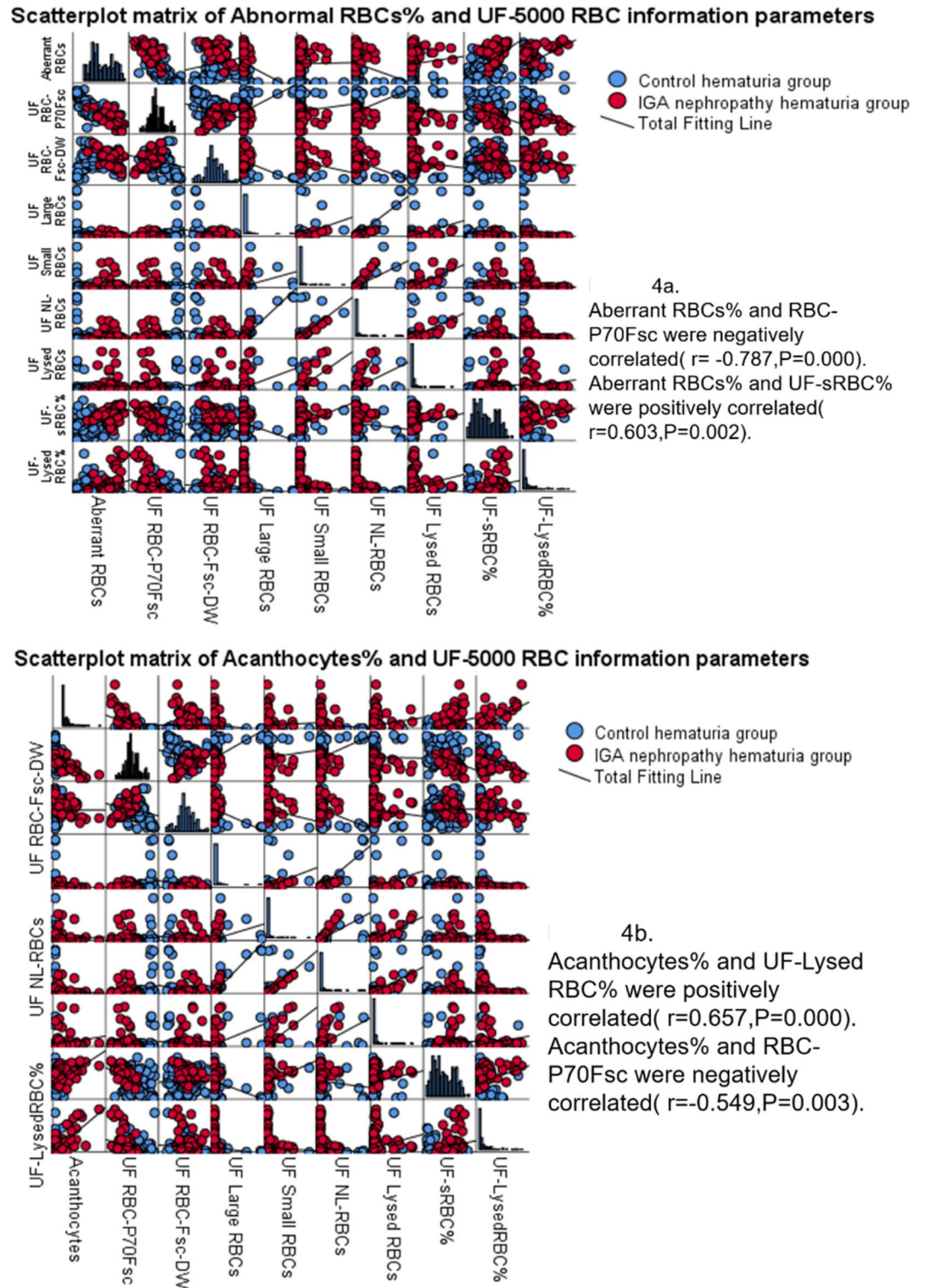


Fig. 4. Correlation scatterplot. Aberrant RBCs% was negatively correlated with RBC-P70Fsc and positively correlated with UF-sRBC%. The acanthocytes% was positively correlated with UF- lysed RBC% and negatively correlated with RBC-P70Fsc. *lysed RBC* lysed red blood cell, *RBC* red blood cell, *UF-sRBC* ratio of small red blood cells to nonlysed red blood cells.

microscopy because it provides fast and convenient erythrocyte information that can be easily standardized in clinical settings.

Methods

Patients and variables

This study was conducted at a 1700-bed general tertiary hospital in China with an ISO 15,189-certified laboratory. According to previous literature studies, > 8000 erythrocytes in the urine, including > 70% dysmorphic RBCs and $\geq 5\%$ acanthocytes, can be used to diagnose glomerular hematuria. Studies that analyzed 238 patients with hematuria found that the use of these values resulted in sensitivity and specificity of 93.10% and 90.16%, respectively. Therefore, we defined the cutoff value for the RBC count as 8000/mL.^{29–31} We enrolled patients with hematuria and urinary erythrocyte counts ≥ 8000 cells/mL³² who presented to our hospital between January 2023 and December 2023. Laboratory data were collected within 2 weeks before renal biopsy, and participants were categorized into the IgAN group (53 participants) or control group (143 participant) based on the renal biopsy results. Inclusion and exclusion criteria for the subgroups were established based on an independent review of clinical data by two experienced physicians in accordance with published guidelines and recommendations^{33,34}. The inclusion criterion for the IgAN group was a histological diagnosis of IgAN determined by the results of a renal biopsy (cases of IgAN in combination with other diseases were excluded). The exclusion criteria were advanced-stage renal diseases and inadequate renal function. The control group inclusion criteria were the identification of urinary system abnormalities via B-mode ultrasound or cystoscopy and/or other urinary causes of hematuria. The exclusion criteria for the control group were the following: histological evidence of glomerular injury confirmed by renal biopsy results; proteinuria (urinary albumin-to-creatinine ratio > 300 mg/g), urine protein > 3000 mg/g, urine protein > 3000 mg/d, or urine protein $\geq 2+$; and urinalysis results indicating blood, granular casts, erythrocytes, and other pathological tubular patterns. Patients with incomplete information and hematuria of unknown origin were excluded, and only the first collected sample was included if multiple samples were collected (Fig. 5). This study was approved by the Institutional Review Board of Dongyang People's Hospital. The Institutional Review Board of Dongyang People's Hospital waived the requirement for informed consent for study participants because this was a retrospective study. All methods of this study were performed in accordance with relevant guidelines and regulations.

Basic demographic data such as sex, age, and urine erythrocyte phase contrast microscopy results, including the urine erythrocyte count (total RBCs), aberrant erythrocyte ratio (aberrant RBCs%), acanthocyte erythrocyte ratio (acanthocytes%), annular erythrocyte ratio (ring forms%), serrated erythrocyte ratio (serrated RBCs%), small erythrocyte ratio (micro-RBCs%), shadow erythrocyte ratio (ghost cells%), and fragmented erythrocyte ratio (fragments%), were collected from both patient groups. The UF-5000 urine sediment analyzer provides information regarding RBC parameters (NLRBCs, lysed RBCs, large RBCs, small RBCs, RBC-P70Fsc, RBC-Fsc-

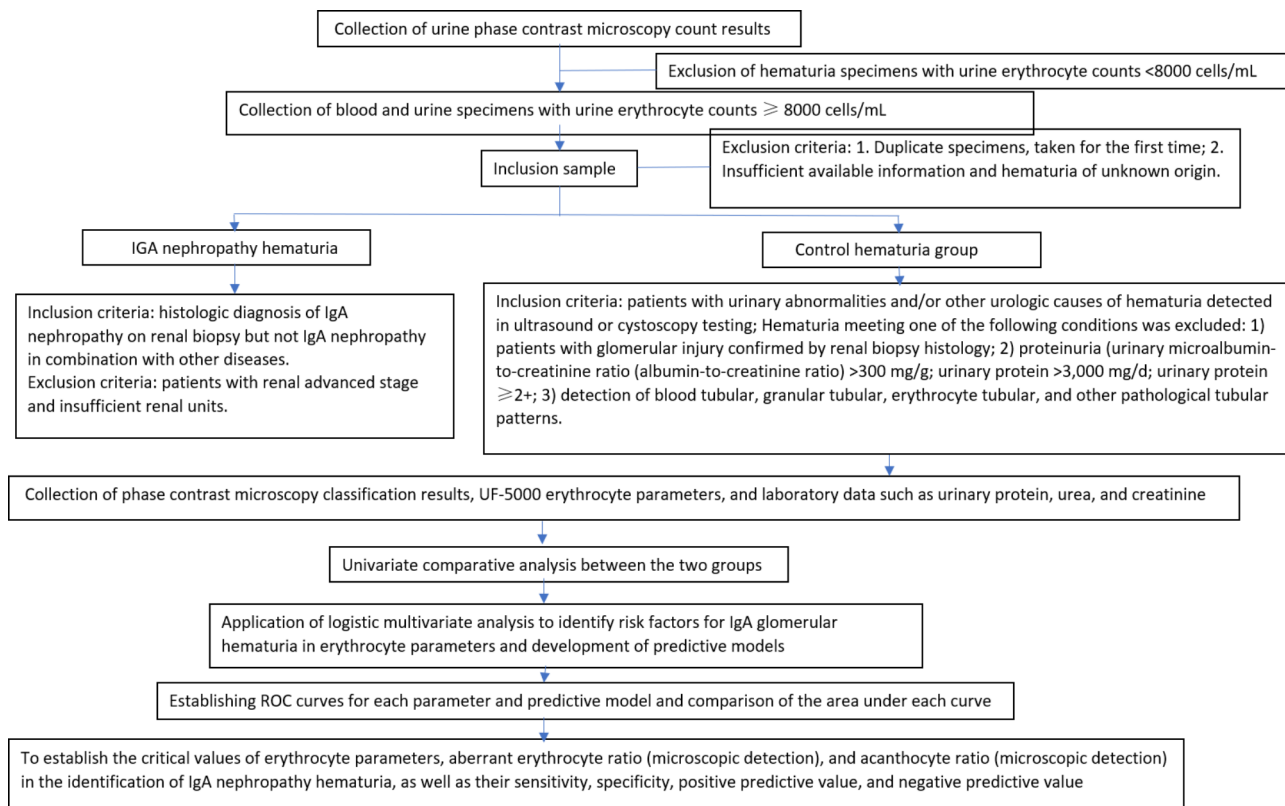


Fig. 5. Flow chart. ROC receiver-operating characteristic.

DW, and RBC-info). The RBC-info parameter categorizes urinary erythrocytes as dysmorphic, isomorphic, and mixed based on RBC-P70Fsc and RBC-Fsc-DW¹⁵. The terms isomorphic-type RBC and dysmorphic-type RBC were used instead of isomorphic RBC and dysmorphic RBC to clarify the autoanalyzer-acquired information about urinary erythrocyte morphology. This helped to avoid confusion related to erythrocyte morphology during urinary sediment analyses. The study also included laboratory data such as the urine protein dry chemistry, blood urea level, blood creatinine level, and estimated glomerular filtration rate.

Urine erythrocyte phase contrast microscopy

The patients were instructed to collect 10 mL of fresh mid-stream urine in a clean and dry urinary catheter. Strenuous exercise was not allowed before collection. The sample was divided into two aliquots: one for the phase contrast microscopy and the other for the routine urinalysis. For phase contrast microscopy, the urine was mixed and erythrocytes were counted using an abalone counting board. Aberrant erythrocytes were categorized based on morphology and counted to determine their percentage in the urine sample. According to the Chinese Expert Consensus on the Nomenclature and Reporting of Results of Urine Organic Fractions, urinary aberrant erythrocytes were categorized as acanthocytes (Fig. 6A), serrated RBCs (Fig. 6B), ring forms (Fig. 6C), ghost cells (Fig. 6C), fragments (Fig. 6C), and micro-erythrocytes (Fig. 6D). Bacillary erythrocytes, sprouting erythrocytes, and spiny erythrocytes were collectively referred to as acanthocytes. Wheel-shaped erythrocytes were termed serrated erythrocytes (serrated RBCs). Bagel-like erythrocytes were categorized as annular erythrocytes (ring forms). Ghost erythrocytes and phantom erythrocytes were classified as shadow erythrocytes (ghost cells). Testing was performed independently by two trained laboratory staff member (aberrant erythrocyte ratio = sum of the number of acanthocytes, serrated RBCs, ring forms, ghost cells, fragments, and micro-erythrocytes/total number of erythrocytes $\times 100\%$; acanthocytes ratio = acanthocytes/total number of erythrocytes $\times 100\%$).

UF-5000 urine organic fraction analysis

The retained urine of the participants was tested using the UC-3500 automatic urine biochemistry analyzer (Sysmex Corporation) and the UF-5000 automatic urine organic fraction analyzer. Urine protein dry chemistry results were automatically read by the UC-3500 automatic urine biochemistry analyzer based on the pH-indicated protein error method. According to the MEDITAPE UC-11 A instruction manual (2021), the reportable ranges of urine protein were as follows: negative; weak positive (15 mg/dL); 1+ (30 mg/dL); 2+ (100 mg/dL); 3+ (300 mg/dL); and 4+ (1000 mg/dL). UF-5000 uses fluorescence flow cytometry to classify urine particles by collecting the following four different signals: forward scattered light, side scattered light, lateral fluorescence, and depolarized side scattered light. Forward scattered light indicates the particle size and permeability, whereas side scattered light provides information regarding the particle thickness and internal structure. Lateral fluorescence indicates particle stainability, and depolarized side scattered light indicates the intensity of particle birefringence. The study parameters of UF-5000 provide necessary information such as the number of undissolved erythrocytes (NLRBCs), large RBCs, small RBCs, lysed RBCs, erythrocyte size index (RBC-P70Fsc), and erythrocyte diversity index (RBC-Fsc-DW). Both RBC-P70Fsc and RBC-Fsc-DW are units of "ch", which is a unit of measurement that reflects the intensity of the forward-scattered light signal. Additionally, we introduced two parameters, the lysed erythrocyte ratio (UF- lysed RBC%) and small erythrocyte ratio (UF-sRBC%), using the following formulas: UF- lysed RBC%=(lysed RBCs/NLRBCs) $\times 100\%$ and UF-sRBC%=(small RBCs/NLRBCs) $\times 100\%$.

Blood biochemical tests

Blood creatinine and urea nitrogen levels in serum were measured after centrifugation at 3000 rpm for 5 min using a LABOSPECT 008AS (Hitachi, Tokyo, Japan). The estimated glomerular filtration rate was determined

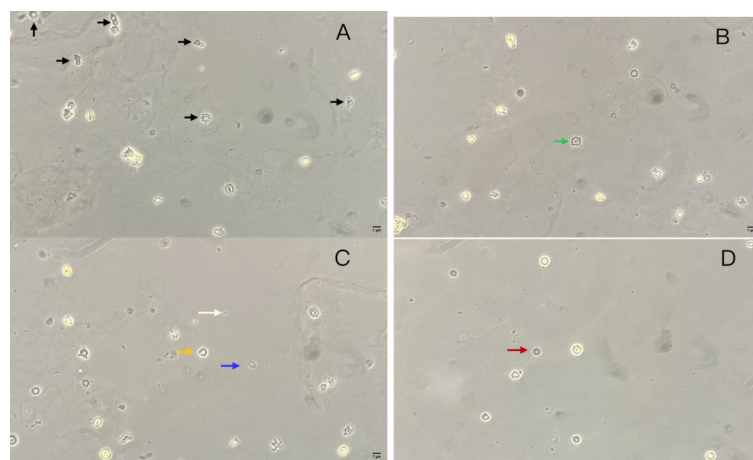


Fig. 6. Aberrant erythrocytes on phase contrast microscopy. (A) Acanthocytes (black arrow). (B) Serrated erythrocyte (green arrow). (C) Ringed erythrocyte (yellow arrow), ghost cell (blue arrow), and erythrocyte fragment (white arrow). (D) Micro-erythrocyte (red arrow).

Name	Meaning	Assignment
Y-Kidney biopsy	Grouping is based on kidney biopsy results	Non-IgA renal hematuria = 1; IgA renal hematuria = 2
X-RBC-P70Fsc	Indicator of urine red blood cell size in UF-5000	Continuous variable, in ch
X-Small RBCs	Indicators of small red blood cells in UF-5000	Continuous variable, in ch
X-Lysed RBCs	Indicators of lysed red blood cells in UF-5000	Continuous variable, in ch
X-UF-sRBC%	Small RBC count (/μL) × 100/NL-RBC count (/μL) in UF-5000	Continuous variable, in %
X-UF-Lysed RBC%	Lysed-RBC (/μL) × 100/NL-RBC count (/μL);	Continuous variable, in %
X-RBC-Info	UF-5000 indicates erythrocyte morphology	Categorical variables, Isomorphic type RBC = 1, Dysmorphic type RBC = 2, mixed type RBC = 3
X-Urine protein	Urinary dipstick scores of protein	Categorical variables, negative = 1, weak positive = 2, 1 + = 3, 2 + = 4, 3 + = 5, 4 + = 6

Table 3. Assignments and variables of risk factors for IgA renal hematuria. UF-sRBC%, Small RBCs/NL-RBCs* 100%; UF-Lysed RBC%, Lysed RBCs/NL-RBCs* 100%; Ch is a unit of measurement used to measure the intensity of a forward scattering light signal.

using the following formula³⁵: estimated glomerular filtration rate (mL/min/1.73 m²) = 194 × serum creatinine (mg/dL) – 1.094 × age (years) – 0.287. For female participants, this value was multiplied by 0.739.

Quantification and statistical analysis

One-way comparative analysis

The statistical analysis and data visualization were performed using SPSS 26.0. The Kolmogorov–Smirnova test was used to assess normality. Normally distributed quantitative data are expressed as means ± SDs, and an independent sample t-test was performed to compare the two groups. Non-normally distributed quantitative data are expressed as IQRs, and the Mann–Whitney test was performed to compare the two groups. Categorical data were analyzed using the chi-squared test or Fisher’s exact probability method. Spearman’s correlation analysis was performed to determine the correlation between erythrocyte parameters and the proportion of urinary aberrant erythrocytes. Statistical significance was set at $P < 0.05$.

Logistic multifactor analysis

A logistic regression analysis was performed to identify risk factors for IgA glomerular hematuria by using grouped variables as dependent variables and selecting statistically significant UF-5000 urinary erythrocyte parameters from the univariate analysis as independent variables (Table 3). Because of the association between urinary protein and the development of IgAN^{6,25,36–38}, we combined the erythrocyte information parameters with the urinary protein dry chemical results to establish a prediction model for glomerular hematuria with IgAN and evaluated the goodness of fit of the model using the Hosmer–Lemeshow test. Statistical significance was set at $P < 0.05$.

ROC analysis

Cutoff values and the corresponding sensitivity, specificity, PPV, and NPV of the respective variables were determined by establishing the working curves. The AUCs of erythrocyte parameters and that of the combined model were compared with that of the manually categorized proportion of aberrant erythrocytes and acanthocytes using the Delong test. Statistical significance was set at $P < 0.05$.

Data availability

The datasets used and analyzed during the current study are available from the corresponding author upon reasonable request.

Received: 27 May 2024; Accepted: 3 January 2025

Published online: 07 January 2025

References

1. Lai, K. N. et al. IgA nephropathy. *Nat. Rev. Dis. Primers.* **2**, 1–20 (2016).
2. Gleeson, P. J., O’Shaughnessy, M. M. & Barratt, J. IgA nephropathy in adults—treatment standard. *Nephrol. Dialysis Transplantation.* **38**, 2464–2473 (2023).
3. Stamellou, E. et al. IgA nephropathy. *Nat. Rev. Dis. Primers.* **9**, 1–21 (2023).
4. Pitcher, D. et al. Long-term outcomes in IgA Nephropathy. *Clin. J. Am. Soc. Nephrol.* **18**, 727–738 (2023).
5. El Karoui, K., Fervenza, F. C. & De Vriese, A. S. Treatment of IgA nephropathy: a rapidly evolving field. *J. Am. Soc. Nephrol.* **35**, 103–116 (2024).
6. Zand, L., Fervenza, F. C. & Coppo, R. Microscopic hematuria as a risk factor for IgAN progression: considering this biomarker in selecting and monitoring patients. *Clin. Kidney J.* **16**, ii19–ii27 (2023).
7. Moreno, J. L. et al. Extracapillary proliferation scoring correlates with renal outcome and contributes to stratification in adult patients with immunoglobulin A nephropathy. *Clin. Kidney J.* **14**, 284–290 (2021).
8. Bobart, S. A. et al. The association of microhematuria with mesangial hypercellularity, endocapillary hypercellularity, crescent score and renal outcomes in immunoglobulin A nephropathy. *Nephrol. Dial Transpl.* **36**, 840–847 (2021).
9. Saha, M. K. et al. Glomerular hematuria and the utility of urine Microscopy: a review. *Am. J. Kidney Dis.* **80**, 383–392 (2022).

10. Hamadah, A. M. et al. Urinalysis for the diagnosis of glomerulonephritis: role of dysmorphic red blood cells. *Nephrol. Dial Transpl.* **33**, 1397–1403 (2018).
11. Martinez, M. G. et al. Comparison of different methods of erythrocyte dysmorphism analysis to determine the origin of hematuria. *Nephron Clin. Pract.* **128**, 88–94 (2014).
12. Ohsaki, H. et al. Diagnostic value of urine erythrocyte morphology in the detection of glomerular disease in SurePath[™] liquid-based cytology compared with fresh urine sediment examination. *Cytopathology* **24**, 52–57 (2013).
13. Mizuno, G. et al. Evaluation of red blood cell parameters provided by the UF-5000 urine auto-analyzer in patients with glomerulonephritis. *Clin. Chem. Lab. Med.* **59**, 1547–1553 (2021).
14. Cwiklińska, A. et al. The results of external quality assessment programme on urine leukocyte and erythrocyte counting in Poland. *Biochem. Med. (Zagreb)*. **30**, 020707 (2020).
15. Nakayama, A., Tsuburai, H., Ebina, H. & Kino, F. Outline and features of UF-5000, fully automated urine particle analyzer. *Sysmex J. International*. **28**, 21 (2018).
16. Cho, H. et al. Diagnostic characteristics of urinary red blood cell distribution Incorporated in UF-5000 for differentiation of glomerular and non-glomerular hematuria. *Ann. Lab. Med.* **42**, 160–168 (2022).
17. Enko, D. et al. Comparison of the diagnostic performance of two automated urine sediment analyzers with manual phase-contrast microscopy. *Clin. Chem. Lab. Med.* **58**, 268–273 (2020).
18. Taguchi, T., von Bassewitz, D. B., Grundmann, E. & Takebayashi, S. Ultrastructural changes of glomerular basement membrane in IgA nephritis: relationship to hematuria. *Ultrastruct Pathol.* **12**, 17–26 (1988).
19. Fünfstück, R. et al. Dysmorphic erythrocytes in glomerulonephritis. 1. Electron microscopical and histochemical investigation. *Cell. Mol. Biol. (Noisy-le-grand)*. **40**, 1113–1124 (1994).
20. Kitamoto, Y., Yide, C., Tomita, M. & Sato, T. The mechanism of glomerular dysmorphic red cell formation in the kidney. *Tohoku J. Exp. Med.* **167**, 93–105 (1992).
21. Hematology and Fluidology Group of the Chinese Society of Laboratory Medicine. Expert Consensus on the naming and reporting of Formative Components of urine tests. *Chin. J. Lab. Med.* **44**, 574–586 (2021).
22. Fanliang, K. Advances in clinical research on urinary erythrocyte morphology and its related parameters. *China Med. Device Inform.* **26**, 20–21 (2020).
23. Costa, R. S. et al. Evaluation of erythrocyte morphology in the urinary sediment for the differential diagnosis of haematurias using standard light microscopy. *Nephrology* **2**, 181–185 (1996).
24. Fogazzi, G. B. et al. Urine erythrocyte morphology in patients with microscopic haematuria caused by a glomerulopathy. *Pediatr. Nephrol.* **23**, 1093–1100 (2008).
25. Gutiérrez, E. et al. Long-term outcomes of IgA nephropathy presenting with minimal or no proteinuria. *J. Am. Soc. Nephrol.* **23**, 1753–1760 (2012).
26. Hamadah, A. M. et al. Urinalysis for the diagnosis of glomerulonephritis: role of dysmorphic red blood cells. *Nephrol. Dialysis Transplantation*. **33**, 1397–1403 (2018).
27. Rath, B., Turner, C., Hartley, B. & Chantler, C. What makes red cells dysmorphic in glomerular haematuria? *Pediatr. Nephrol.* **6**, 424–427 (1992).
28. Köhler, H., Wandel, E. & Brunck, B. Acanthocyturia—a characteristic marker for glomerular bleeding. *Kidney Int.* **40**, 115–120 (1991).
29. Fudong, L. et al. Application of urine erythrocyte phase detection in the differential diagnosis of kidney disease. *Mod. J. Lab. Med.* **04**, 64–65 (2008).
30. Xiao, X., Rengao, Y. & Wengong, J. Clinical evaluation of urine erythrocyte phase microscopy in the diagnosis of glomerular hematuria. *Chin. J. Integr. Traditional Western Med. Nephrol.* **03**, 146–148 (2004).
31. Sanghong, L. et al. A new urinary red blood cell differential calculation method to identify the source of hematuria. *Chin. J. Intern. Med.* **04**, 255–258 (1994).
32. Lifang, H. & Chenyu, L. Fundamentals of Clinical Testing, Fourth Edition. Beijing. *People's Medical Publishing House* 4, 174–175 (2007).
33. Barocas, D. A. et al. Microhematuria: AUA/SUFU Guideline. *J. Urol.* **204**, 778–786 (2020).
34. Hebert, L. A., Parikh, S., Prosek, J., Nadasdy, T. & Rovin, B. H. Differential diagnosis of glomerular disease: a systematic and inclusive approach. *Am. J. Nephrol.* **38**, 253–266 (2013).
35. Matsuo, S. et al. Revised equations for estimated GFR from serum creatinine in Japan. *Am. J. Kidney Dis.* **53**, 982–992 (2009).
36. Oortwijn, B. D. et al. Demonstration of secretory IgA in kidneys of patients with IgA nephropathy. *Nephrol. Dial Transpl.* **22**, 3191–3195 (2007).
37. Haq, K. & Patel, D. M. Urinalysis: interpretation and clinical correlations. *Med. Clin. North. Am.* **107**, 659–679 (2023).
38. Chen, X. et al. Proteomic profiling of IgA nephropathy reveals distinct molecular prognostic subtypes. *iScience* **26**, 105961 (2023).

Acknowledgements

We would like to thank Editage (www.editage.cn) for English language editing.

Author contributions

SL developed the study concepts and design. XL, CC, LC, DZ collected the data. XH analyzed and interpreted the data. JZ wrote the manuscript. All authors read and approved the final manuscript.

Declarations

Competing interests

The authors declare no competing interests.

Additional information

Correspondence and requests for materials should be addressed to S.L.

Reprints and permissions information is available at www.nature.com/reprints.

Publisher's note Springer Nature remains neutral with regard to jurisdictional claims in published maps and institutional affiliations.

Open Access This article is licensed under a Creative Commons Attribution-NonCommercial-NoDerivatives 4.0 International License, which permits any non-commercial use, sharing, distribution and reproduction in any medium or format, as long as you give appropriate credit to the original author(s) and the source, provide a link to the Creative Commons licence, and indicate if you modified the licensed material. You do not have permission under this licence to share adapted material derived from this article or parts of it. The images or other third party material in this article are included in the article's Creative Commons licence, unless indicated otherwise in a credit line to the material. If material is not included in the article's Creative Commons licence and your intended use is not permitted by statutory regulation or exceeds the permitted use, you will need to obtain permission directly from the copyright holder. To view a copy of this licence, visit <http://creativecommons.org/licenses/by-nc-nd/4.0/>.

© The Author(s) 2025